

The MyShake App: User Experience of Early Warning Delivery and Earthquake Shaking

Sarina C. Patel¹  and Richard M. Allen¹ 

Abstract

MyShake is a free citizen science and public safety smartphone application that delivers the United States ShakeAlert program's Earthquake Early Warning to the public in the states of California, Oregon, and Washington. Although smartphone notifications have long been a component of the ShakeAlert warning delivery plan, very little data has been published on the efficiency and accuracy of such communication. MyShake records timestamps in its alert processing system, including the time it takes for a phone to receive and acknowledge an alert's delivery. We use data collected for five representative earthquakes—three in urban regions, two rural events—since October 2019 to assess MyShake alert delivery latencies and ground-motion prediction accuracy. For these events, MyShake was capable of efficiently processing and delivering warnings. For the smaller urban events that occur beneath the target population, about half of recipients received a warning before the estimated onset of the S-wave, and up to 90% received an alert prior to experiencing peak shaking. When earthquakes occur further from populated areas, the warning time naturally increases. Smartphone acceleration recordings can also be used to quantify the user experience during earthquakes because they are colocated with people. A review of waveforms collected by MyShake shows a systematic amplification of shaking recorded by smartphones relative to nearby traditional stations. The median amplification calculated using records from all five sample events is a factor of 3.1. Once this correction is applied, MyShake peak accelerations are generally consistent with the distribution of shaking intensities in the U.S. Geological Survey ShakeMap product, whereas also showing some individual sites with substantial amplification and de-amplification. In addition to delivering early warnings, therefore, MyShake provides a waveform observation dataset to densify shaking intensity observations and thereby improve our understanding of earthquake effects and evaluate the accuracy of ShakeAlert's alerting regions.

Cite this article as Patel, S. C., and R. M. Allen (2022). The MyShake App: User Experience of Early Warning Delivery and Earthquake Shaking, *Seismol. Res. Lett.* **XX**, 1–13, doi: [10.1785/SRL20220062](https://doi.org/10.1785/SRL20220062).



[Supplemental Material](#)

Introduction

Public earthquake early warning systems are expanding around the globe (Allen and Melgar, 2019; Allen and Stogaitis, 2022). To be effective, however, they require a reliable and efficient method of delivering alerts to private citizens in the seconds available before shaking is felt. Alarms on television and radio, personal devices, and a public siren system are all mass distribution systems used globally (Hoshiba, 2014; Allen *et al.*, 2018; Given *et al.*, 2018). Alerts can also be sent to individuals via automated email subscriptions, SMS, and in the age of the smartphone, as an app notification. When the United States ShakeAlert system began public alerting across all of California in October of 2019, FEMA's Wireless Emergency Alerts—commonly known for distributing Amber Alerts for missing children—were designated the default delivery method because it is a function native to phones sold in the United States, although there were concerns about alert delivery speed (Given *et al.*,

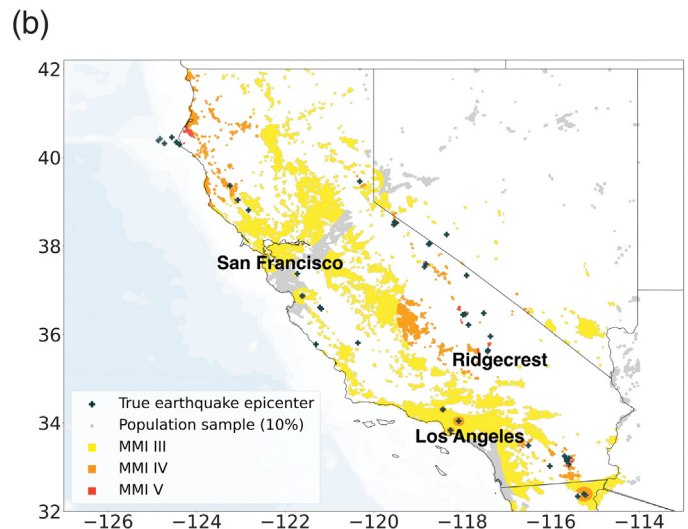
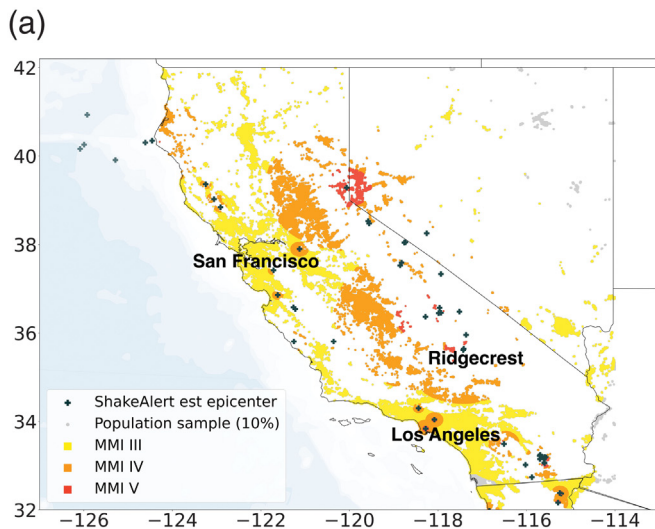
2018; Kohler *et al.*, 2020). Since the 2019 launch, alerts have also been delivered via smartphone app notifications, which permit greater flexibility in how the alert is presented and how a user can interact with the information. Little data existed, however, to quantify the actual effectiveness and efficiency of delivering early warning as app notifications in the context of existing network technologies.

MyShake is a free earthquake app that began as a citizen science project in 2016 (Kong, Allen, and Schreier, 2016; Kong, Allen, Schreier, and Kwon, 2016). The app provides near-real-time earthquake information to the user, as do many apps.

1. Berkeley Seismological Laboratory, University of California, Berkeley, Berkeley, California, U.S.A.,  <https://orcid.org/0000-0003-2212-9908> (SCP);  <https://orcid.org/0000-0003-4293-9772> (RMA)

*Corresponding author: sarina.patel@berkeley.edu

© Seismological Society of America



Uniquely, MyShake also records earthquake shaking during an event. This is accomplished using the accelerometer built into all smartphones. An onboard machine learning-trained classifier identifies when shaking is likely from an earthquake. It then sends that waveform data to an archive for research. This provides instrumental records of the shaking at the location of the phone such as in an office or home. As such, it can provide uniquely dense data on the shaking experience of people in the built environment.

For the 2019 ShakeAlert launch in California, MyShake added the ability to deliver alerts to become the state of California's official early warning app supported by the Governor's Office of Emergency Services (CalOES). Since then, MyShake has delivered one or more ShakeAlerts to nearly every part of the state (Fig. 1). Alert delivery was extended to the state of Oregon in March 2021, and to Washington in January 2022. As part of its function as an alert provider, MyShake has internally tracked the latency of its entire system, from the receipt of a ShakeAlert message by a MyShake server through to alert delivery on individual smartphones, to quantify the system's warning delivery efficiency and identify avenues for improvement. To our knowledge, MyShake is the only earthquake app to continuously monitor and report such data. Brooks *et al.* (2021) quantify delivery latency using test "alerts" sent to a cluster of 15 phones located close together in San Juan, Costa Rica, and found an average 4 s delivery latency. However, they acknowledge such a small sample size and distribution region may not be representative of more deliveries for a real earthquake over a wide region. Other research on smartphone earthquake early warning latency considers the time to detection and alert generation, but neglects the time required for delivery (Kong *et al.*, 2020; Bossu *et al.*, 2021). Google began delivery of early warning in the United States in 2020 and is piloting smartphone-detected early warning in New Zealand, Greece, Turkey, the Philippines, Kazakhstan, Kyrgyz Republic, Tajikistan, Turkmenistan, and Uzbekistan, however, delivery latency data has not been published.

Figure 1. Maps showing alert regions across California through the end of April 2022. (a) Essentially all of California has been sent at least one alert. The points on the maps mark the distribution of a random 10% sampling of California's population to show where people tend to be located. Population points in yellow have received a public alert and were in a region expected to experience Modified Mercalli Intensity (MMI) III shaking for at least one event. Orange represents MMI IV and red represents MMI V. The map on the left shows the location and alert area for the largest ShakeAlert-estimated magnitude alert associated with each of the 48 events for which ShakeAlert has issued an alert $>M$ 4.5 prior to 2022. (b) The right side map represents the true locations of the earthquakes and what the alert area would have been if the magnitude estimate had been exactly correct.

In this article, we use the data retained by MyShake to analyze the speed and ground-motion accuracy at which ShakeAlert earthquake early warnings can be delivered to affected populations via app notification. We find that alerts reach the majority of individuals prior to their experience of peak shaking. MyShake's citizen science collection of acceleration data during earthquakes can also be used as a window into the user experience during earthquakes. In general, we find that smartphones record a higher acceleration than either the predicted ground motion or actual ground motions recorded at local traditional stations. We suggest this amplification might be accounted for by considering both the frequencies of building response and site-specific ground-motion amplification effects.

MyShake

MyShake is a free, publicly available, citizen science earthquake app for both Android and Apple smartphones. Since its inception in 2016, the app has been downloaded globally over 1.6 million times. Public facing features include a map and custom notification service for global earthquakes, safety and preparedness information, community-sourced experience reports, education materials to view real waveforms, and, in the states

(a) MyShake • now ^
 Earthquake - Drop, cover, hold on. Shaking expected.
 Mag 6.2 eq at 12:00 PM PST on Tue Feb 19 - via ShakeAle..

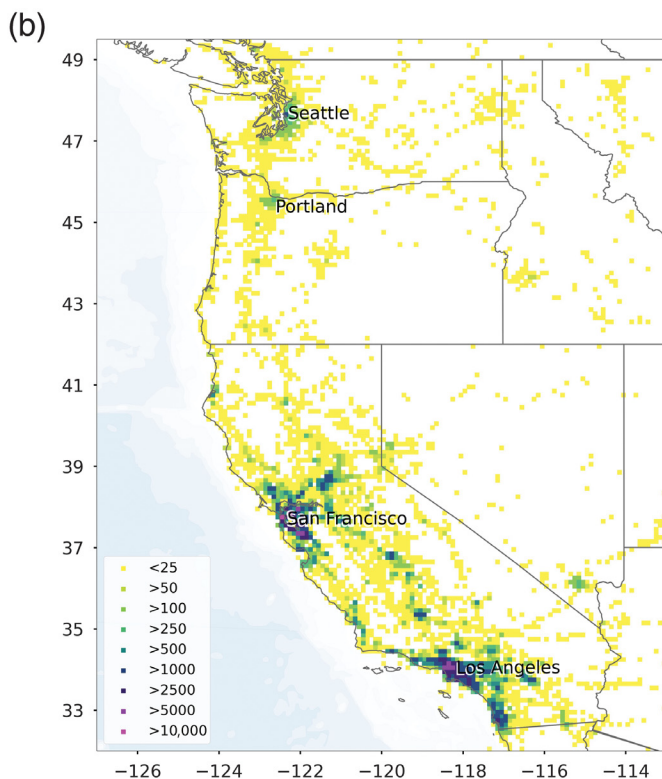


Figure 2. (a) An example of the alert message sent to MyShake users during an earthquake and (b) a registration density map for MyShake downloads in the western United States, binned into 10 km squares. MyShake provides public alerts in the three western coastal states of Washington, Oregon, and California.

of California, Oregon and Washington, earthquake early warning alerts and follow-up information (Fig. 2). Citizen science features include parametric data (such as short-term average/long-term average [STA/LTA] triggers) collected on the phone and transmitted to a central server for use in real time, and waveform records from the phone's onboard accelerometer collected in near-real time. Real-time data includes small "heartbeat" messages, which contains items such as triggering information when an earthquake is detected using the onboard algorithm, and receipt timestamps when the phone receives an alert from the MyShake server. Being small, heartbeats are transmitted immediately upon creation to MyShake servers

using whatever transmission method is available to the phone. The app minimizes the power consumption and transmission stress of larger packets of data, such as full waveforms when an earthquake is detected, by waiting until the phone is connected to power and WiFi.

The scientific core of MyShake is a machine learning algorithm that distinguishes between earthquake shaking and human activity with 93% accuracy (Kong, Allen, Schreier, and Kwon, 2016). When a phone is stationary and not in use, the app monitors the onboard accelerometer for earthquake-like motion. When such motion is detected, a trigger heartbeat is sent to a central server and the app retains a 5 min waveform to be transmitted when power and connectivity requirements are met. Waveforms can also be recorded when prompted by the receipt of an early warning message.

Early Warning Alerts

The United States early warning system is ShakeAlert, which is operated by the U.S. Geological Survey (USGS) in collaboration with the regional seismic networks, and with support in California from CalOES. In accordance with USGS thresholds, ShakeAlerts are distributed to private smartphones located in regions predicted to experience Modified Mercalli Intensity (MMI) III (weak shaking) or greater for earthquakes estimated by ShakeAlert to be magnitude 4.5 or greater (Kohler *et al.*, 2020). ShakeAlert approximates MMI distribution using a ground-motion prediction equation (GMPE) that ingests the estimated magnitude value and produces intensity radii around the estimated epicentral location—or around an estimated fault length if the event is large enough (Kohler *et al.*, 2020). The MMI III region is defined by the MMI 2.5 computed radius. Upon detecting an event, an alert message is sent from ShakeAlert to the MyShake backend system, which then determines which users' locations fall within the MMI III radius and should receive the alert. The alert leaves the MyShake servers to be transmitted via cell tower and WiFi service to users.

When MyShake receives and begins processing a ShakeAlert, it retains a "processing-start" timestamp (t_0). Timestamps for each targeted phone are also recorded at successive transition points in the backend processing system until the alert is forwarded to the distribution system, Firebase, for transmission to phones (t_3). We refer to the interval it takes the MyShake servers to process the alert and push it to distribution (t_3-t_0) as the Server Processing Time. The messages travel via cell network and internet to reach target phones. When a phone receives the alert, it records the receipt time (t_7) and reports it back to the MyShake servers for delivery confirmation. We refer to the interval from when MyShake received an alert until the phone received the alert as the Alert Acknowledgement Time (t_7-t_0).

During an earthquake, ShakeAlert often sends a sequence of alert updates. The MyShake backend fully processes one ShakeAlert update before seeking the most recent update

TABLE 1

Alert Delivery Latencies Associated with Three Urban and Two Rural Earthquakes at the Alert Delivery Level of MMI III

Date	Magnitude	Event	Region	Depth (km)	Initial Mag Est.	Max Mag Est.	Time between 1st and Max Est. (s)	Alerts Sent	Percentile	t3-t0	t7-t0
										(s)	(s)
2020/09/19	M 4.5	El Monte	Los Angeles area	17	M 4.5	M 4.8	7.73	20,169	20%	1.39	0.74
									50%	1.84	1.88
									80%	2.59	3.50
2020/09/18	M 4.3	Carson	Los Angeles area	12	M 4.7	M 4.9	0.53	25,018	20%	1.07	1.30
									50%	1.81	2.21
									80%	3.17	5.06
2021/06/03	M 3.6	Alum Rock	Southern Bay Area	7	M 4.5	M 4.5	n/a	8097	20%	0.97	1.19
									50%	2.18	2.41
									80%	3.87	4.06
2020/06/04	M 5.5	Searles Valley	Ridgecrest aftershock	8	M 5.7	M 5.8	1.50	20,825	20%	2.90	2.62
									50%	4.53	4.73
									80%	6.92	7.85
2020/06/24	M 5.8	Lone Pine	Ridgecrest aftershock	5	M 5.0	M 6.2	44.44	47,747	20%	5.42	5.21
									50%	6.79	7.18
									80%	8.54	9.50

Alert delivery latencies associated with three urban and two rural earthquakes at the alert delivery level of MMI III. The “Alerts Sent” column indicates how many unique phones were identified as falling within the alerting region, processed by the server, and sent an alert. Each of the righthand time columns is the equivalent of the Server Processing Time (t3-t0) and Alert Acknowledgement Time (t7-t0), respectively, in which t3 and t7 are measured on each phone and t0 is the time MyShake began processing the alert update that first included that phone. Latency values are provided for the 20th, 50th, and 80th percentiles for each earthquake.

(with the assumption that ShakeAlert’s accuracy generally improves with time and increasing quantities of data) and calculates whether any additional phones should be alerted. Once MyShake has alerted a given region, it will skip reprocessing that region during subsequent alert updates, so our total “Alerts Sent” count for each earthquake does not contain duplicates to the same device.

In addition to real events, MyShake’s alerting system is tested daily with “silent” alerts. The system is fed a test alert message and performs the full delivery process to phones but does not show users a visible message. The majority of these silent tests check MyShake’s large-scale delivery capacity using a scenario magnitude 7.5 earthquake centered under an urban region of California.

Latency Data

We present the latency for five of the most significant earthquake alerts delivered to date in California as representative examples of MyShake’s alert delivery efficiency in Table 1. Three of these earthquakes occurred beneath urban areas, where the window to alert the nearest population center was small, and two are rural events. The urban events occurred in the Los Angeles and San Jose areas of California. All are relatively small events (M 4.5 El Monte, M 4.3 Carson, and M 3.6 Alum Rock) that ShakeAlert estimated to be at least an M 4.5, which triggered a public alert. The rural events were both aftershocks of the 2019 Ridgecrest earthquakes in southeastern California. They were somewhat larger in magnitude (M 5.5 Searles Valley and M 5.8 Lone Pine), and the MMI III alert

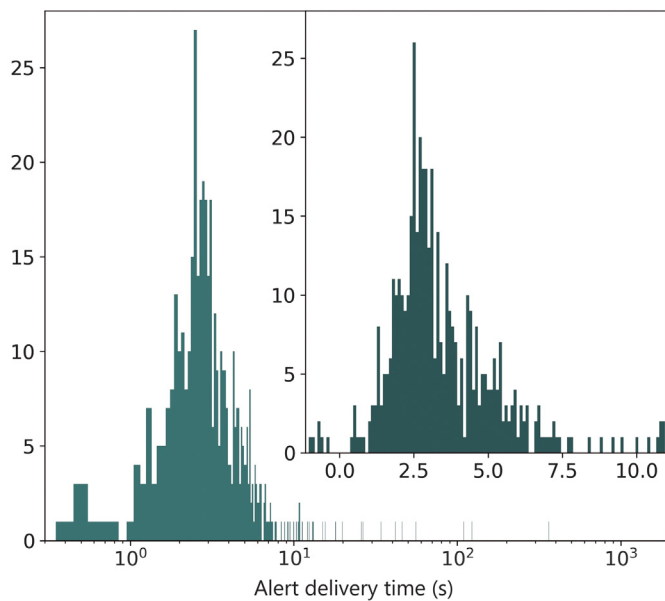


Figure 3. Histogram showing the distribution of the Alert Acknowledgement Time (t_7-t_0 , binned by 0.1 s) for the **M** 4.3 Carson earthquake, from the 2nd to the 99th percentile on a log scale in the larger window, and the 1st to 85th percentile on a linear scale in the inset. Beyond these boundaries are a handful of anomalous records.

region extended into the Los Angeles basin, some 200 km away. An example of the full distribution of the time to delivery (t_7-t_0) is shown for the most recent event, (**M** 4.3 near Carson, California) in Figure 3.

Outside factors that can influence latency include: whether users are located in an area with poor reception, whether a phone is connected to WiFi or cellular data, and how the Firebase messaging service employed by MyShake balances its bandwidth against message volume. Another issue is the accuracy of the timestamps recorded on the phones for alert acknowledgement. Previous research has shown that 75% of timestamps reported by phones differ from true server time by 0–1.6 s (Kong *et al.*, 2019). Because phone clocks can be both ahead or behind true time, some Alert Acknowledgement times

will be shorter than expected, making the 20th percentile times lower, and some timestamps will be later, making the 80th percentile value higher. The consistency of the median (50th percentile) t_7-t_0 for each event being slightly larger than the median t_3-t_0 time corroborates previous observations that phone time error is distributed around zero. Not all phones provide delivery receipts. This is due to messaging prioritization “features” of the operating systems, connectivity issues, and data security features on phones.

Monitoring system latency has lent insight toward opportunities for improvement. One important improvement made to the system was branching the data processing into three parallel “shards” that can process a batch of phones each, simultaneously. Implemented for the purposes of load balancing and efficient scalability as usership grows, this sharding went live on 25 June 2020. The improvement to server processing speed can be viewed in Table 1 when comparing the results for the 19 September 2020 El Monte event to the 4 June 2020 Searles Valley Ridgecrest aftershock, for which comparable numbers of phones were sent an alert. For the post-sharding El Monte event, the speed-up was about 5 s. As usership grows, additional shards are added to maintain efficiency.

User Experience of Warning Time

To better understand the user experience, we consider the MyShake phones that both recorded waveform data and returned a receipt after receiving an early warning alert (or for which the vibration from the alert is visible in the waveform itself, such as in Fig. 4). The waveform data are three orthogonal components of acceleration collected using the onboard accelerometer and encompasses 1 min prior and 4 min following an activation prompt to begin recording. All waveforms used for analysis are visually verified by a seismologist so that spurious nonearthquake signals are not included. To determine warning times, we subtract the alert delivery time from either the estimated *S*-wave arrival time, or the observed occurrence of peak shaking recorded by the same phone. We use both time measurements to quantify how much warning time users were given to respond.

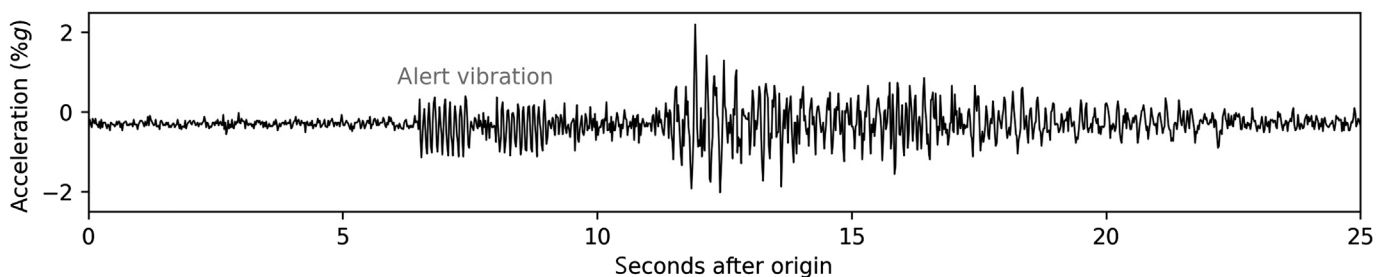


Figure 4. The vibration of the alert arriving overprints the horizontal component of a phone recording the *P*-wave arrival 29 km

from the epicenter of the **M** 4.5 El Monte event in September 2020. The alert arrives 5 s before peak shaking is recorded.

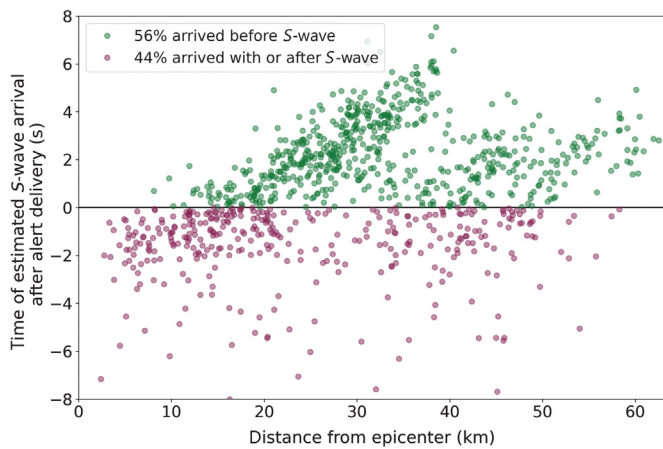


Figure 5. Alert delivery times for the September 2020 **M** 4.5 El Monte earthquake, represented as the time that phones at various epicentral distances received the alert relative to the estimated *S*-wave arrival time. The green points above the central line have a positive warning time. *S*-wave velocity is estimated to be 3.5 km/s (Lin et al., 2010).

The Los Angeles (El Monte and Carson) and southern Bay Area (Alum Rock) events represent the most challenging alerting cases. There is a small alerting area (due to the small magnitudes), a large population to warn, and a hypocenter directly beneath the population. For all three, about half of alerted users received an alert before the estimated arrival of the *S*-wave (Fig. 5). Being 17 and 12 km deep, the Los Angeles earthquakes gave users a slightly longer lead time than the 7 km deep Alum Rock event, resulting in closer to 60% of users with a pre *S*-wave alert time versus 40% (Carson and Alum Rock versions of Fig. 5 are included as Figs. S1b and S3b in the supplemental material, available to this article).

In the case of the **M** 4.5 El Monte earthquake, ShakeAlert produced an initial magnitude estimate of **M** 4.5, prompting the first set of alerts represented by the earlier linear trend in Figure 5 out to 37 km. Then, 7.7 s later, ShakeAlert estimated the event to be a **M** 4.8, causing a new set of alerts for phones further away, represented by the second linear trend.

Peak acceleration was measured using waveforms collected by phones that also returned an alert delivery receipt (Fig. 6a). Figure 6b shows the shaking intensity measured by each phone (peak acceleration to intensity scaling is discussed in the [User Experience of Intensity](#) section) in the **M** 4.5 El Monte earthquake and also the time at which the peak shaking occurred relative to the origin time of the earthquake. Figure 6c subtracts the alert delivery time from the peak shaking time so that the warning time until peak shaking is shown. In the case of the El Monte event, 90% of phones received 0–10 s warning. The expansion of the alerting area at 7.7 s is visible in the handful of phones in Figure 6c that are further away from the event

but have shorter warning times between the alert delivery and observation of peak shaking. For the **M** 3.6 Alum Rock earthquake in the southern Bay Area, about half of alerted users received a warning of 0–10 s before experiencing peak shaking. About three quarters of the phones had 0–15 s warning before peak shaking in the **M** 4.3 Carson event. Figures like Figure 6 for the other events can be found as Figures S2, S4, and S6. As intensity attenuates with distance, the longest warning times naturally tend to occur for the lower intensities.

We consider the geographic distribution of alert deliveries over time, relative to the ShakeAlert alerting extents for the **M** 4.5 El Monte and **M** 5.8 Lone Pine events (Fig. 7). Each point represents a phone, which is colored by the time of alert delivery relative to the time that ShakeAlert produced its first alert. The concentric circles represent alerting regions computed using ShakeAlert’s successive magnitude estimates, beginning with the red circle at the center and going out to the largest alerting region encircled by yellow. For the El Monte event, the 7.7 s delay between the first and largest estimates is evidenced by the color shift between the inner and outer circles. ShakeAlert can update its magnitudes several times over the course of a single event. For clarity, only a subset of these estimates is plotted in these figures.

For the **M** 5.8 Lone Pine event (Fig. 7b), the estimated magnitude grew several times, causing multiple iterations of alert deliveries by MyShake. The initial estimate was **M** 5 (alerting area represented by the inner red circle). The estimate grew to **M** 5.6 four seconds later, and a **M** 5.8 six seconds after that. The largest estimate, **M** 6.2 was generated 44 s after the initial alert, causing the distinct color difference in delivery times at the center of the map relative to the edges. Even with this much later alert, the phones alerted at the greatest distance received almost a minute of warning. For depictions of alert delivery times for the Carson, Alum Rock, and Searles Valley events, see Figures S1a, S3a, and S5a respectively.

Two Ridgecrest aftershocks, one **M** 5.8 in Lone Pine on 4 June 2020 and the second **M** 5.5 in Searles Valley on 24 June 2020, demonstrate the longer warning times that are possible for larger magnitude earthquakes. In these events, users received up to a minute of warning time prior to shaking (Fig. 8a; Fig. S5b). Because of the rural location of the epicenter, nearly all users also experienced positive warning time prior to the occurrence of peak shaking at their location (Fig. 8b,c; Fig. S6d,e). Although warning times are expected to be greatest in further away, lower intensity shaking regions, at least one phone recording an estimated MMI V peak shaking intensity ~100 km from the epicenter received ~16 s of warning.

User Experience of Intensity

Because MyShake phones receiving alerts can also record the shaking during the earthquake, we can make in situ observations about user experiences of shaking and intensity. Companion research has found remarkable correlation between intensity

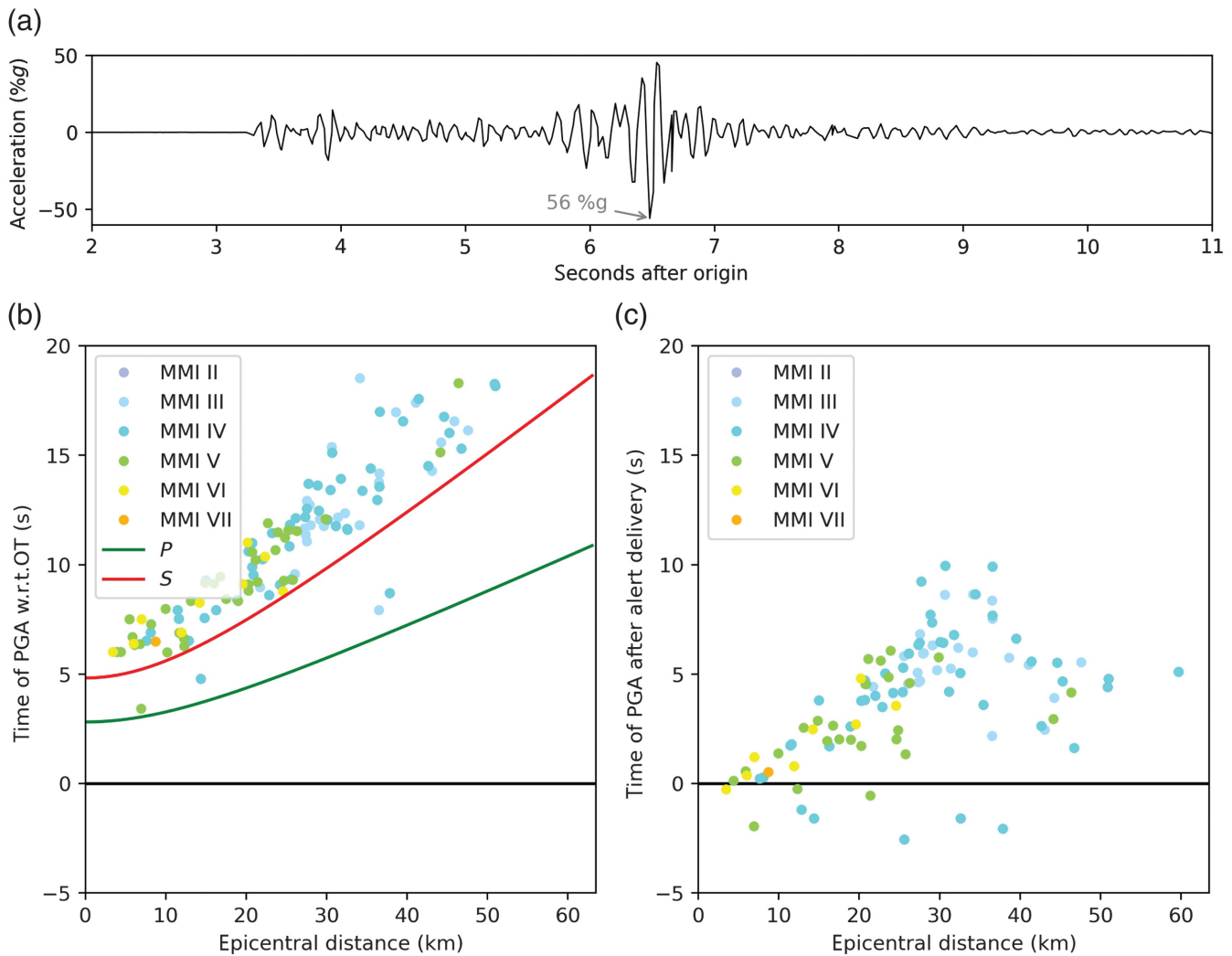


Figure 6. Peak ground shaking and alert delivery times for the **M** 4.5 September 2020 El Monte earthquake (a) the largest amplitude acceleration waveform recorded at ~ 10 km (represented by the orange MMI VII dot in panels b and c). (b) The time and distance of phones when they recorded the maximum acceleration, with a ShakeMap color scheme to denote intensity. Peak acceleration is scaled to intensity using the MyShake scaling factor and the Worden *et al.* (2012) relationship (see the [User experience of intensity](#) section). *P*-wave speed is approximated as 6 km/s (Lin *et al.*, 2010) and *S*-wave speed is computed as 60% of *P*. (c) The time that phones at various epicentral distances recorded peak acceleration relative to the time of receiving an early warning.

maps generated using MyShake’s simple user experience survey versus the USGS Did You Feel It? survey (Kong *et al.*, 2022). Here, we use waveform data to compare to the USGS ShakeMap product. The Modified Mercalli Intensity scale represents shaking severity, which can be estimated from peak ground acceleration (PGA) and peak ground velocity (PGV) recordings using the Worden *et al.* (2012) relationship, which is an empirical scaling relation determined by comparing PGA and PGV from seismometers coupled directly with the ground to proximal human reports of ground shaking intensity collected through Did You Feel It? However, the Worden relationship was developed for traditional seismic data. Phones, meanwhile, typically exist within the built environment, such as within a building. With their greater freedom of motion, buildings typically experience higher amplitude motion than the free ground surface. Therefore, we must revisit the PGA to MMI scaling relation before we can apply it to phone observations. To do this we first compare the accelerations recorded by phones and the traditional stations contributing to ShakeMap for each of the five sample events (Fig. 9). We find that phones at a given epicentral distance record peak accelerations that are greater than both the PGA recorded by traditional stations at

the same distance and the accelerations predicted by the Boore *et al.* (2014) (“BSSA14”) GMPE for shallow, crustal earthquakes in the western United States (Fig. 9).

To quantify the amplification, we bin phones and traditional stations by epicentral distance in 5 km increments and compute the ratio of the peak accelerations recorded by each (Fig. 10a). In aggregate across the five sample events and all epicentral distance bins, we find the median of the ratio of MyShake to traditional station accelerations is 3.1. This

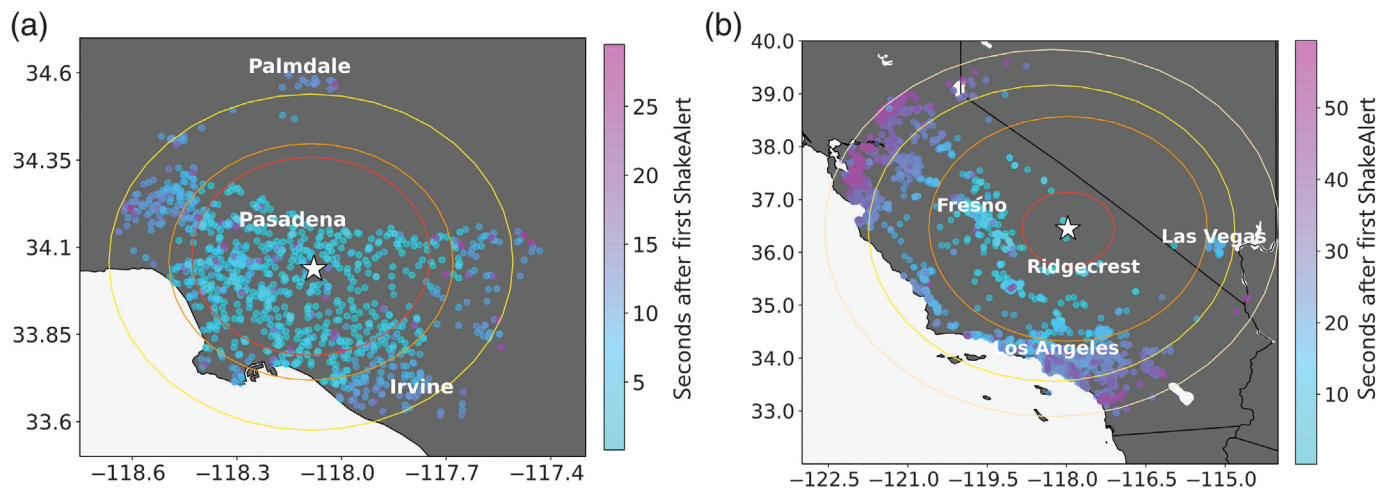
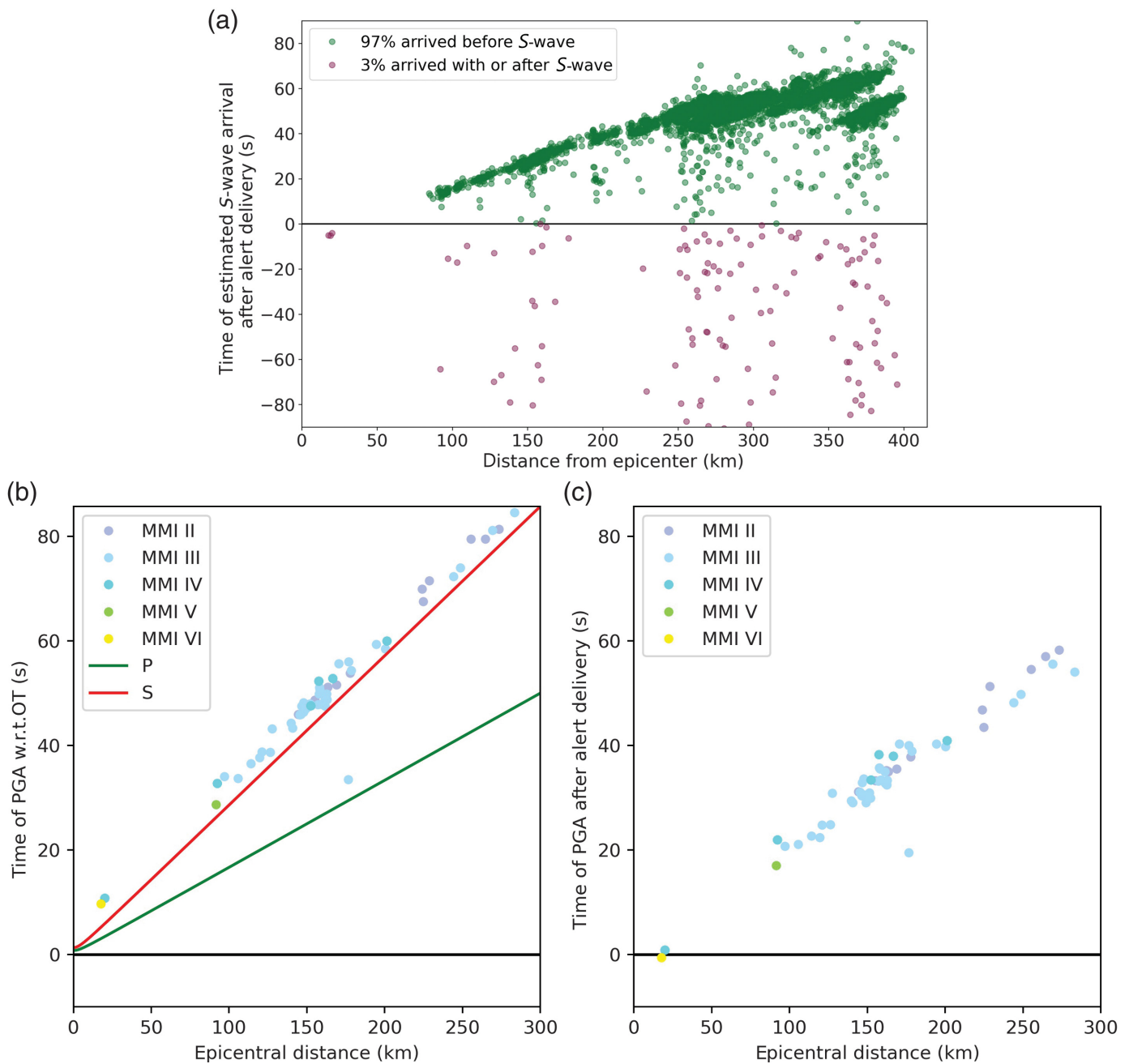


Figure 7. (a) A map of alert delivery times for the September 2020 **M** 4.5 El Monte event, within 30 s of ShakeAlert producing its first alert (initial alerting radius marked by the red circle). The largest estimate (yellow circle) occurred 7.7 s after the initial. (b) A map of alert delivery times for the June 2020 **M** 5.8 Lone Pine earthquake within 55 s of ShakeAlert producing its first alert. The colors of the circles representing key evolutions in the ShakeAlert magnitude estimate—and therefore alert radii—are ordered in rainbow sequence by time, beginning with red. The initial (red) estimate was **M** 5. A **M** 5.6 estimate followed 4 s later, and an **M** 5.8 was produced 10 s after the first estimate. The final **M** 6.2 estimate occurred 44 s after the first.

amplification cannot be explained by variability in phone quality, as the standard deviation of the log of phone peak acceleration in each bin is typically lower than that of the traditional station PGAs (Fig. 10c). Therefore, there is a real amplification of shaking consistently being recorded by MyShake phones relative to traditional sensors. Buildings amplify shaking relative to the free surface at the natural resonance frequencies of the structure (Chopra, 2012). Because phones are typically located inside buildings, some of the MyShake amplification is likely due to structural features. The fundamental period of a building is typically close to the number of floors times 0.1 s (Lee *et al.*, 2003; Dym and Williams, 2007). Based on the geographic distribution of MyShake users, we assume the majority are located in single family homes or low-rise apartment buildings, for which the resonance period would be in the 0.1 to 0.3 s range. Therefore, we compare MyShake peak acceleration to pseudospectral acceleration (PSA) at 0.3 s, which is also provided for these events by the USGS ShakeMap product. When we compare the ratio of MyShake PGA to traditional station PSA at 0.3 s, we find a median ratio of 1.7 (Fig. 10b). This is lower than the factor of 3.1 when comparing MyShake peak acceleration to traditional PGA, but also suggests that the acceleration amplification due to buildings alone cannot explain the full amplification effect. Possible additional causes of this amplification include hyper-local near-station site effects, the fact that most population centers (and thus phones and buildings) are in sedimentary basins that amplify shaking (Parker and Baltay, 2022), and the resonance of the furniture on which the phones are located.

Given the observed amplification effect, we first correct MyShake waveform accelerations by dividing by our preliminary correction factor 3.1 to better represent a traditional seismometer PGA, and then apply the relationship defined by equation (3) and the coefficients from table 1 in Worden *et al.* (2012) to determine MMI. This allows us to approximate the MMI for a given MyShake peak acceleration observation and compare it with other observations and estimates of MMI, for example, with an earthquake’s computed ShakeMap.

ShakeMap derives shaking intensity distribution from a combination of traditional seismic data translated to intensity using the Worden relationship and crowd-sourced Did You Feel It reports (Atkinson and Wald, 2007). Intensity is a human-centric metric of impact. Because ShakeMaps are calibrated with reports of real experiences, they are a reliable depiction of shaking intensity for an event for which there are observations. We compare MyShake observations of intensity to ShakeMap intensity contours (Fig. 11). The two sets of intensity estimates are as consistent as we would expect. Not all MyShake observations fall within their corresponding intensity contours, but ShakeMap contours are themselves smoothed representations of heterogeneous data too; some number of individual traditional station observations often deviate from the contours. Our conclusion, therefore, is that MyShake acceleration data can add granularity to our understanding of the heterogeneity of ground motion and user intensity experience. This is not only of intrinsic value but can also provide constraints on alert accuracy and event impact severity, especially in urban areas where densifying observations can improve the quality of situational awareness products. We find both instances of greater-than-expected-intensity, by as much as two MMI units for MyShake phones compared to ShakeMap contours, and instances of reduced, lower-than-expected intensity. For example, Figure 6a shows the waveform



for the phone that reached MMI VII peak acceleration (after application of the MyShake correction factor) in the **M** 4.5 El Monte event, yet there is no MMI VII contour depicted on the ShakeMap (Fig. 11a). Visual inspection of the waveform confirms that the peak shaking is earthquake-related and not spurious noise. The conclusion, therefore, is that although the event was relatively small, some users still experienced notably high intensities. In a larger, damaging event, extra high intensity measurements could be used to help emergency response target more heavily impacted structures. Other waveforms for surprisingly high and low accelerations can be found in Figures S2, S6, and S7.

Figure 8. Alert delivery times for the June 2020 **M** 5.8 Lone Pine earthquake. Similar plots for the June 2020 **M** 5.5 Searles Valley earthquake can be found in Figure S6. (a) Warning time represented as the time that phones at various epicentral distances received an alert relative to the estimated arrival of the *S*-wave. The alert updates that promoted the expansion of the alerting region can be seen in the parallel diagonal linear trends at further distances. The green points above the central line have a positive warning time. (b) The time and distance of phones when they recorded the peak acceleration, with a ShakeMap color scheme used to denote intensity. (c) The time that phones at various epicentral distances recorded peak acceleration relative to the time of receiving an early warning.

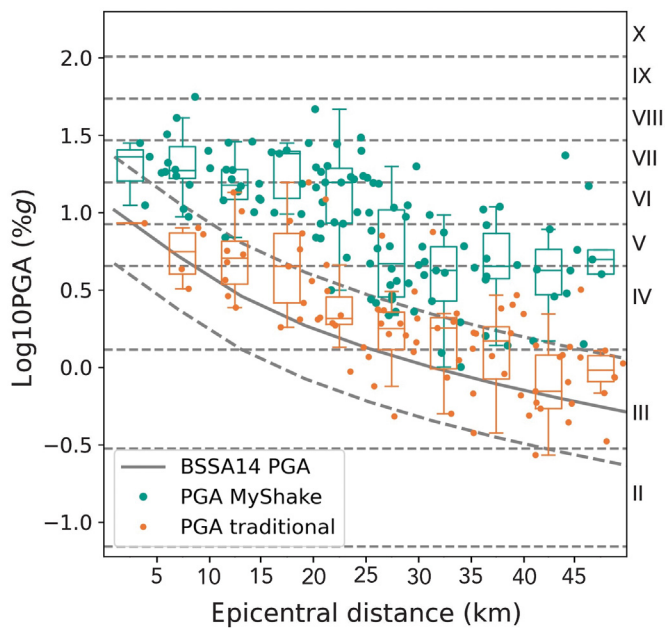


Figure 9. Peak acceleration recorded by traditional stations (orange) and MyShake phones (teal) for the **M** 4.5 El Monte event. Individual observations are shown as points, and the box plots show the distribution for waveforms collected within each 5 km epicentral distance bin. The gray curve represents the prediction based on the [Boore et al. \(2014\)](#) ground-motion model (BSSA14) with dashed lines \pm one standard deviation. The right side y-axis shows approximate equivalent MMI levels.

Summary

Although delivering early warning alerts to private individuals via smartphones has been a long-term goal within the ShakeAlert project (e.g., [Given et al., 2018](#)), there were few published empirical measurements to assess exactly how efficient and effective such an alerting method could be in the context of the United States ShakeAlert system. By tracking the latencies and alert deliveries by MyShake in its first two years of operation as a public warning service, we can confirm that MyShake is capable of delivering timely warning such that the majority of users receive an alert prior to experiencing peak shaking intensity, even for small magnitude earthquakes beneath urban centers when the available warning time is minimal. As expected, warning time is greater when events occur outside population centers or when the magnitude is large. Also as expected, warning times for an individual event are greatest where epicentral distances are largest, and therefore tend to vary inversely with shaking intensity. It is worth noting, however, that in a large earthquake, higher intensity shaking will have a broader distribution. Thus, even with the latency induced short-to-late alert zone, many strong shaking regions have the potential to receive alerts in a useful timeframe.

MyShake waveforms also show accelerations greater than predicted using a standard GMPE, and greater than

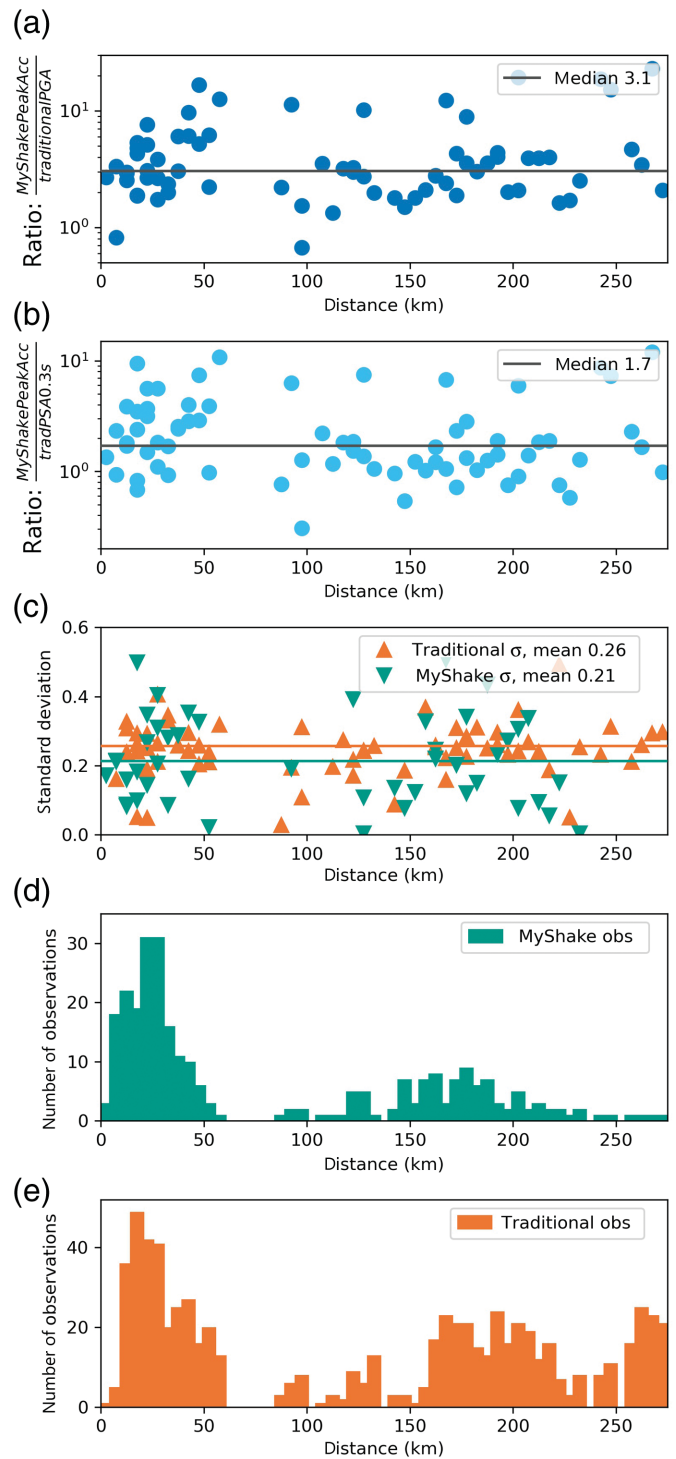
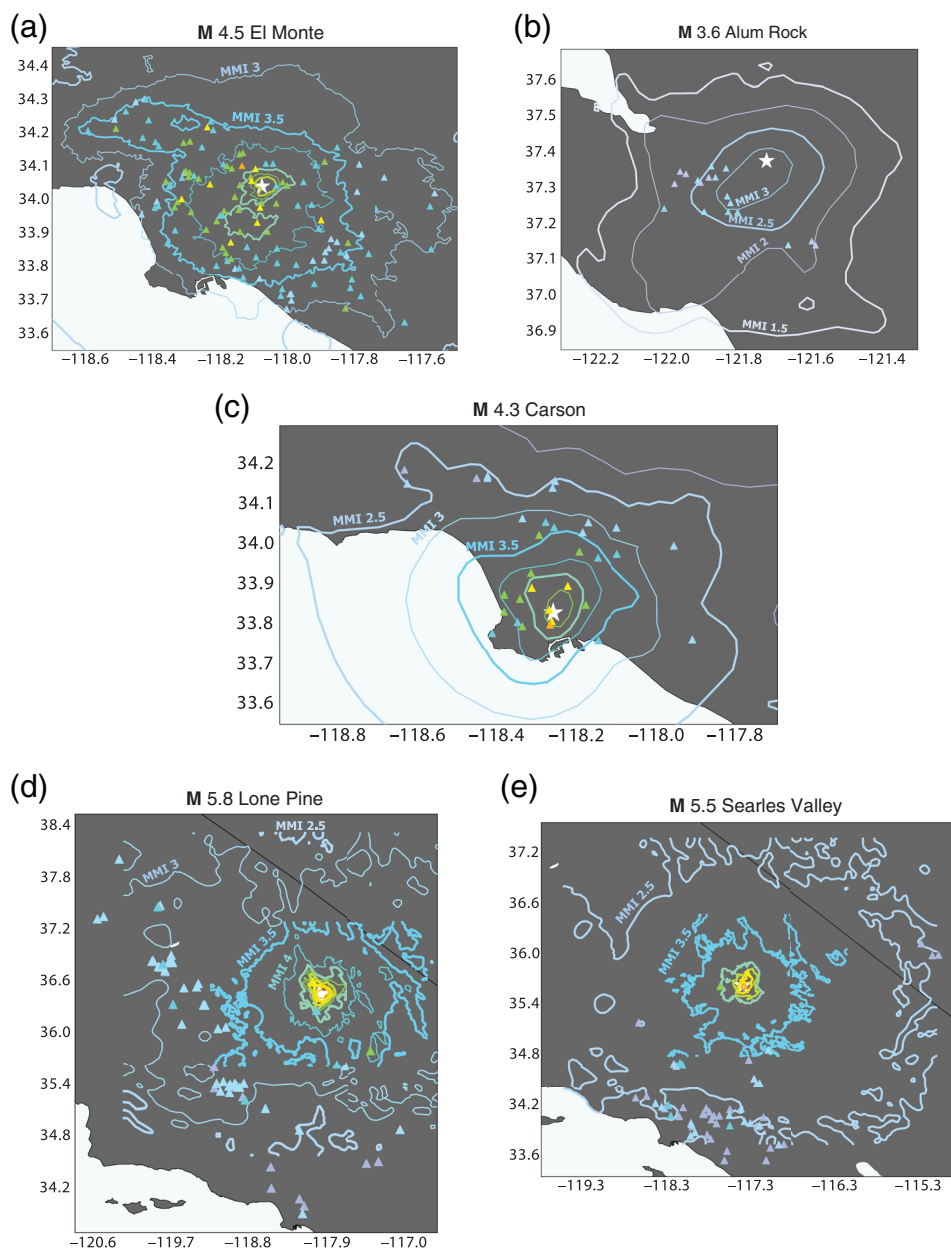


Figure 10. (a) The ratio of MyShake peak acceleration versus traditional station peak ground acceleration (PGA), as binned over 5 km increments for the five sample events. (b) The ratio of MyShake peak acceleration versus 0.3 s pseudospectral acceleration (PSA) from traditional stations. (c) The standard deviation of the log10 of MyShake and traditional station peak acceleration measurements. (d) The number of MyShake observations for all events binned by epicentral distance. (e) The number of traditional station observations for all events binned by epicentral distance.



Perceived shaking	Not felt	Weak	Light	Moderate	Strong	Very strong	Severe	Violent	Extreme
Potential damage	None	None	None	Very light	Light	Moderate	Mod./Heavy	Heavy	Very heavy
Peak acc (%g) trad. stations	<0.05	0.3	2.8	6.2	12	22	40	75	>139
Peak acc. (%g) MyShake	<0.15	0.9	8.6	19	37	68	123	230	>427
Instrumental intensity	I	II-III	IV	V	VI	VII	VIII	IX	X+

Scale adapted from Worden *et al.* (2012)

Figure 11. Maps of the U.S. Geological Survey (USGS) ShakeMap contours overlaid by intensity measurements made by MyShake phones, marked by triangles colored using the Worden *et al.* (2012) conversion and the MyShake Correction Factor. Only phones that returned a waveform we could use to make an intensity measurement are plotted. (a) The September 2020 **M** 4.5 El Monte event; (b) the June 2021 **M** 3.6 Alum Rock event; (c) the September 2021 **M** 4.3 Carson event; (d) the June 2020 **M** 5.8 Lone Pine Ridgecrest aftershock; and (e) the June 2020 **M** 5.5 Searles Valley Ridgecrest aftershock. There are multiple ShakeMap versions available for each event; we present the maps produced by the most recent software iteration. For panels (d) and (e), however, the latest software version sets default area limits which exclude the lower intensity contours. We include MMI 2.5 and 3 contours from a less preferred ShakeMap version from the National Earthquake Information Center (NEIC), to provide an approximate sense of scale.

traditional stations nearby. This is likely due to local site effects and structural amplification of the built environment. Comparisons with local seismic stations recording peak ground acceleration leads to a median amplification factor of 3.1; comparison with response spectra at a period of 0.3, which may be closer to a building's response, yields a median conversion factor of only 1.7. Although derived using limited data, we find reasonably good correlation between MyShake data divided by this correction factor and the ShakeMaps for each of the five sample events. Therefore, with this preliminary correction factor, MyShake data can be incorporated into the larger discussion of the shaking experienced by users relative to expected or estimated intensities. Because phones are located where users are, MyShake's intensity observations inherently improve the shaking resolution where such granularity is most useful.

Over the course of operations as a public emergency notification service, the public has mostly responded favorably to receiving early warnings, with little concern expressed for overalerting, such as when the magnitude is overestimated by ShakeAlert. One contribution to this may be that users seem to expect an alert anytime they feel shaking, as opposed to shaking of a specific threshold, as noted in Cochran and Husker (2019) and MyShake user feedback via email and Twitter. As ShakeAlert operation continues in the future, MyShake data can provide information on both the

alerting timeline and the experience level of ground motion. This information can help us optimize the alerting strategy for ShakeAlert and other Earthquake Early Warning systems around the world.

Data and Resources

For user privacy reasons, data collected by MyShake are stored securely at UC Berkeley and are not publicly available for analysis. Information about ShakeAlert warning parameters was also sourced through the MyShake alert distribution system. Traditional station data and ShakeMaps were downloaded from the U.S. Geological Survey (USGS) ShakeMap repository. Data for individual events can be found on their respective event pages at earthquake.usgs.gov. Maps and Figures are plotted in Python using the Matplotlib and Cartopy packages (J. D. Hunter, “Matplotlib: A 2D Graphics Environment”, *Computing in Science & Engineering*, vol. 9, no. 3, pp. 90–95, 2007; Cartopy, v0.17.0 downloaded 30 January 2020. Met Office, United Kingdom, available at <https://scitools.org.uk/cartopy/docs/latest/>). Maps also made with Natural Earth. Free vector and raster map data available at naturalearthdata.com. ShakeMap data accessed through the USGS at <https://earthquake.usgs.gov/data/shakemap/>. All figures in the supplemental material are versions of the figures present in the main article, except using the data from other earthquakes discussed in the text, and as such utilize no additional resources. All websites were last accessed in May 2022.

Declaration of Competing Interests

The authors acknowledge that there are no conflicts of interest recorded.

Acknowledgments

The authors are grateful for the contributions and support from current and former MyShake team and Berkeley Seismology Lab members for their assistance on this work: Jennifer Strauss, Stephen Thompson, Stephen Allen, Akie Mejia, Theron Bair, Qingkai Kong, Angela Lux, Roman Baumgaertner, Garner Lee, Arno Puder, Louis Schreier, Kaylin Rochford, Sharon Pothan, Doug Neuhauser, Stephane Zuzlewski, and Asaf Inbal. The authors thank all the MyShake user citizen scientists for their data contributions. The authors also thank our reviewers Annemarie Baltay and John Vidale for their thoughtful feedback and time. This work was funded by the California Governor’s Office of Emergency Services (Cal OES), Agreement Number 6142-2018.

References

Allen, R. M., and D. Melgar (2019). Earthquake early warning: Advances, scientific challenges, and societal needs, *Annu. Rev. Earth Planet. Sci.* **47**, no. 1, doi: [10.1146/annurev-earth-053018-060457](https://doi.org/10.1146/annurev-earth-053018-060457).

Allen, R. M., and M. Stogaitis (2022). Global growth of earthquake early warning, *Science* **375**, no. 6582, 717–718.

Allen, R. M., E. S. Cochran, T. J. Huggins, S. Miles, and D. Otegui (2018). Lessons from Mexico’s earthquake early warning system, *Eos Earth Space Sci. News* **99**, doi: [10.1029/2018EO105095](https://doi.org/10.1029/2018EO105095).

Atkinson, G. M., and D. J. Wald (2007). “Did You Feel It?” intensity data: A surprisingly good measure of earthquake ground motion, *Seismol. Res. Lett.* **78**, no. 3, 362–368.

Boore, D. M., J. P. Stewart, E. Seyhan, and G. M. Atkinson (2014). NGA-West2 equations for predicting PGA, PGV, and 5% damped PSA for shallow crustal earthquakes, *Earthq. Spectra* **30**, no. 3, 1057–1085, doi: [10.1193/070113EQS184M](https://doi.org/10.1193/070113EQS184M).

Bossu, R., F. Finazzi, R. Steed, L. Fallou, and I. Bondár (2021). “Shaking in 5 Seconds!”—Performance and user appreciation assessment of the earthquake network smartphone-based public earthquake early warning system, *Seismol. Res. Lett.* **93**, no. 1, 137–148, doi: [10.1785/0220210180](https://doi.org/10.1785/0220210180).

Brooks, B. A., M. Protti, T. Ericksen, J. Bunn, F. Vega, E. S. Cochran, C. Duncan, J. Avery, S. E. Minson, E. Chaves, *et al.* (2021). Robust earthquake early warning at a fraction of the Cost: ASTUTI Costa Rica, *AGU Adv.* **2**, no. 3, 1–17, doi: [10.1029/2021av000407](https://doi.org/10.1029/2021av000407).

Chopra, A. (2012). *Dynamics of Structures: Theory and Applications to Earthquake Engineering*, Prentice Hall, San Francisco.

Cochran, E., and A. Husker (2019). How low should we go when warning for earthquakes? *Science* **366**, no. 6468, doi: [10.1126/science.aaz6601](https://doi.org/10.1126/science.aaz6601).

Dym, C. L., and H. E. Williams (2007). Estimating fundamental frequencies of tall buildings, *J. Struct. Eng.* **133**, no. 10, 1–5.

Given, D. D., R. M. Allen, A. S. Baltay, P. Bodin, E. S. Cochran, K. Creager, R. M. de Groot, L. S. Gee, E. Hauksson, T. H. Heaton, *et al.* (2018). Revised technical implementation plan for the ShakeAlert system—An earthquake early warning system for the West Coast of the United States, doi: [10.3133/ofr20181155](https://doi.org/10.3133/ofr20181155).

Hoshiya, M. (2014). Review of the nationwide earthquake early warning in Japan during its first five years, in *Earthquake Hazard, Risk, and Disasters*, Elsevier, 505–529, doi: [10.1016/B978-0-12-394848-9.00019-5](https://doi.org/10.1016/B978-0-12-394848-9.00019-5).

Kohler, M. D., D. E. Smith, J. Andrews, A. I. Chung, R. Hartog, I. Henson, D. D. Given, R. de Groot, and S. Guiwits (2020). Earthquake early warning ShakeAlert 2.0: Public rollout, *Seismol. Res. Lett.* **91**, no. 3, 1763–1775, doi: [10.1785/0220190245](https://doi.org/10.1785/0220190245).

Kong, Q., R. M. Allen, S. Allen, T. Bair, A. Meja, S. Patel, J. Strauss, and S. Thompson (2022). Crowdsourcing felt reports using the MyShake smartphone app, doi: [10.48550/oxford.2204.12675](https://doi.org/10.48550/oxford.2204.12675).

Kong, Q., R. M. Allen, and L. Schreier (2016). MyShake: Initial observations from a global smartphone seismic network, *Geophys. Res. Lett.* **43**, no. 18, 9588–9594, doi: [10.1002/2016GL070955](https://doi.org/10.1002/2016GL070955).

Kong, Q., R. M. Allen, L. Schreier, and Y.-W. Kwon (2016). MyShake: A smartphone seismic network for earthquake early warning and beyond, *Sci. Adv.* **2**, e1501055, doi: [10.1126/sciadv.1501055](https://doi.org/10.1126/sciadv.1501055).

Kong, Q., R. Martin-Short, and R. M. Allen (2020). Toward global earthquake early warning with the MyShake smartphone seismic network, Part 2: Understanding MyShake performance around the world, *Seismol. Res. Lett.* **91**, no. 4, 2218–2233, doi: [10.1785/0220190178](https://doi.org/10.1785/0220190178).

Kong, Q., S. Patel, A. Inbal, and R. M. Allen (2019). Assessing the sensitivity and accuracy of the MyShake smartphone seismic network to detect and characterize earthquakes, *Seismol. Res. Lett.* **90**, no. 5, doi: [10.1785/0220190097](https://doi.org/10.1785/0220190097).

Lee, W. H., H. Kanamori, P. C. Jennings, and C. Kisslinger (Editors) (2003). International handbook of earthquake and engineering seismology, part B, in *International Geophysics*, Vol. 81, Academic Press, London, United Kingdom.

Lin, G., C. H. Thurber, H. Zhang, E. Hauksson, P. M. Shearer, F. Waldhauser, T. M. Brocher, and J. Hardebeck (2010). A California statewide three-dimensional seismic velocity model from both absolute and differential times, *Bull. Seismol. Soc. Am.* **100**, no. 1, 225–240, doi: [10.1785/0120090028](https://doi.org/10.1785/0120090028).

Parker, G. A., and A. S. Baltay (2022). Empirical map-based nonergodic models of site response in the greater Los Angeles area, *Bull. Seismol. Soc. Am.* **112**, no. 3, 1607–1629, doi: [10.1785/0120210175](https://doi.org/10.1785/0120210175).

Worden, C. B., M. C. Gerstenberger, D. A. Rhoades, and D. J. Wald (2012). Probabilistic relationships between ground-motion parameters and modified Mercalli intensity in California, *Bull. Seismol. Soc. Am.* **102**, no. 1, 204–221, doi: [10.1785/0120110156](https://doi.org/10.1785/0120110156).

Manuscript received 28 February 2022
Published online 27 July 2022